LATVIAN JOURNAL OF PHYSICS AND TECHNICAL SCIENCES
2017, N 4

DOI: 10.1515/lpts-2017-0026

STABILITY AND THE ELECTRONIC STRUCTURE OF XB_2 (X = Pt, Ir, Pd, Rh, Os) DIBORIDES

A.I. Popoola, A.Y. Odusote, O.E. Ayo-Ojo
Department of Physics,
Federal University of Technology, Akure, NIGERIA.
Email: ispopoola71@gmail.com

First-principle calculations have been performed to investigate the structural and electronic properties of platinum group metal diborides in the stoichiometry XB_2 (X = Pt, Ir, Pd, Rh, Os). All investigated compounds have shown to belong to the orthorhombic *P*mmn space group rather than the *C*2/m previously predicted in some of the compositions. Compressibility will reduce with boron addition in Pt, Pd and Rh, but will increase with boron addition into Ir and Os. The electronic density of states show that all the compounds are metals, with PtB_2, PdB_2 and OsB_2 being potentially incompressible and superhard materials.

Keywords: *bulk modulus, hardness, machinability, metallic diborides, thermodynamic stability*.

1. INTRODUCTION

Hard materials with high bulk modulus are materials of choice in a wide variety of industrial applications. They are used as abrasives, cutting tools and coatings where wear prevention or scratch resistance is important. Apart from hardness, they have demonstrated exceptional thermal conductivity, refractive index and chemical stability [1], [2]. The development of a new class of hard materials is of prime importance. High valence electron density and bond covalence are required in the creation of ultra-incompressible, hard materials. The valence electron density for diamond, the hardest known substance, is 0.705 electrons/Å^3. It has an exceptionally high bulk modulus B_0 of442 GPa. Covalent bonding dominates in hard materials. Unlike covalent materials, the electrostatic interactions in ionic materials are omni-directional, leading to low bond-bending forces and automatically, to low shear modulus [3], [4]. Hard materials are often plagued by intrinsic brittleness, poor thermal shock resistance and the difficulty of machining into sharp edge/complex shapes.

For platinum group metal related materials, pure Osmium (Os) has exceptionally high (395-462 GPa) bulk modulus, while its hardness is 400 kg/mm^2 [5]. The high bulk modulus of Os can mainly be attributed to its high valence electron density, while its low hardness is related to the metallic bonds and its hexagonal close-packed (HCP) crystal structure. OsB_2 has been synthesized [6], [7]. It is a

highly incompressible (365-395 GPa) and hard (≥2000 kg/mm^2) material [8]. Two different structures, the *P*mmn orthorhombic [9] and the *C*2/m monoclinic [10] have been reported in IrB_2 through *ab initio* density-functional theory calculations. The structure of RhB_2 has also been proposed to be monoclinic at ambient pressure [11].

Platinum, iridium, rhodium and palladium are all neighbours to Os, with high valence electron density. Specifically, the stoichiometry-property data on platinum and palladium borides are scanty. Some of the impressive properties of Pt, Pd, Ir and Rh are: high corrosion resistance, high melting points and good ductility [12]. These impressive properties could predispose them to good compositional design of new metallic borides. It should be noted that, Pt (3.5MPa), Pd (4.75MPa), Rh (6.0MPa) and Ir (6.5MPa) are softer compared to Os (7.0MPa). Evidence has shown that pure but soft transition metals will become hard materials when combined with small covalent bond-forming atoms such as boron, carbon, oxygen, or nitrogen [13], [14], [15]. It should therefore be a worthy adventure to investigate the effect of boron on Pt, Ir, Rh and Pd. The structure of Pt, Rh, Ir and Pd is cubic. Application benefits are expected from these materials and the results could perhaps help predict new phases in Pt, Ir, Os, Rh and Pd diborides. The goal of the present research is to carry out density functional calculations on the electronic properties and the bulk modulus of XB_2 (X = Ir, Os, Pt, Rh, Pd). Where necessary, clarity will be provided between competing structures and new materials will be predicted.

1.1 CRYSTAL STRUCTURE OF METAL DIBORIDES

The widely reported structures for metallic diborides are the AlB_2 (P6/mmm) structure, the monoclinic (*C*2/*m*) structure and the orthorhombic (*P*mmn) structure (Fig. 1). The metals locate at (0,0,0) and boron at (and (Wyckoff positions in the AlB_2 structure, while in the monoclinic structure, metal atoms are at (0.409; 0.00; 0.836) with boron atoms at (0.669; 0.00; 0.488) and (0.708; 0.50; 0.264), respectively. In the orthorhombic structure, the metal atoms locate at (0.25; 0.25; 0.1545) and boron at (0.0557; 0.25; 0.6325) and (0.444; 0.25 0.6325) Wyckoff positions. Our investigation covers all these three structures. However, similarity in atomic packing exists between hexagonal and cubic structures - they both have closed packed planes. Only one plane exists in hexagonal structures, while there are four in cubic structures. Close packed planes predisposes a material to slip, a phenomenon that can be of immense benefits for the mechanical properties of such material. Therefore, a hypothetical cubic phase of the diborides is considered. The adopted cubic structure has slight modification from the hexagonal type, wherein same Wyckoff atomic positions are assumed.

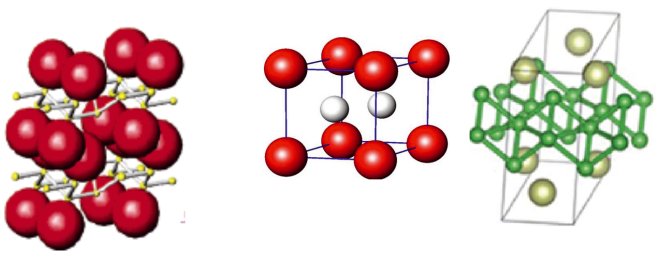

Fig.1. Different structure types in metallic diboride – left: *P*mmn; middle: AlB_2 and right: *C*2/m.

2. CALCULATION METHODS

All numerical calculations were performed using the QUANTUM ESPRESSO (QE) code [16]. QE is a DFT code that uses plane waves as a basis for the wavefunctions and a pseudopotential to treat core electron interactions. The Generalized Gradient Approximation of Perdew-Burke-Ernzerhof [17] was used for the exchange and correlation functional. The following: Ir ($3d^74s^2$), Pt ($4s^24p^1$), Rh ($4d^{10}5s^25p^1$), Pd ($3s^2$ $3p^2$), Os($5s^2$ $5p^2$) and B ($5s^2$ $5p^3$) respectively were treated as valence by the pseudopotentials. The smearing was fixed at 0.06 with the Marzari-Vanderbilt smearing scheme. The k-point sampling in the Brillouin zone (BZ) was performed using the Monkhorst–Pack scheme [18]. The energy-cutoff for the plane-wave basis sets was 75 Ry with 8×5×6, 6×8×7 and Γ-centered Monkhorst–Pack grids conducted for the electronic BZ integrations for the orthorhombic, C2/m and the hexagonal structures, respectively.

Each crystal structure relaxation was carried out with the Broyden-Fletcher-Goldfarb-Shanno (BFGS) minimisation technique. The criteria for convergence in optimising the atomic internal degrees of freedoms were as follows: difference on total energy within 1×10^{-8} Ry/atom, ionic Hellmann-Feynman forces within 0.001 Ry/a.u. Each structure and its internal coordinates were first optimised to get a relaxed structure. The total energy per unit cell as a function of volume was calculated and the results were fitted using the Birch-Murnaghan equation of state (eq. 1) to get the bulk modulus [19]. The step size for volume contraction/expansion was 0.2. About 10 data points, evenly distributed around the equilibrium lattice constant were used.

$$P(V) = \frac{3B_0}{2}\left[\left(\frac{V_0}{V}\right)^{\frac{7}{3}} - \left(\frac{V_0}{V}\right)^{\frac{5}{3}}\right]\left\{1 + \frac{3}{4}\left(B_0' - 4\right)\left[\left(\frac{V_0}{V}\right)^{\frac{2}{3}} - 1\right]\right\} \quad (1)$$

with

$$B_0 = -V\left(\frac{\partial P}{\partial V}\right), \quad (2)$$

where is the isothermal volume, is the isothermal bulk modulus, is the derivative of the bulk modulus with respect to pressure and is the energy of the material which is found by integrating (1) and given as:

$$E(V) = E_0 + \frac{9V_0B_0}{16}\left\{\left[\left(\frac{V_0}{V}\right)^{\frac{2}{3}} - 1\right]^3 B_0' + \left[\left(\frac{V_0}{V}\right)^{\frac{2}{3}} - 1\right]^2\left[6 - 4\left(\frac{V_0}{V}\right)^{\frac{2}{3}}\right]\right\} \quad (3)$$

The formation energy ($\Delta E^{\ominus}$), is traditionally used to gauge if a substance can be made by conventional means. $\Delta E^{\ominus}$ is the energy of XB_2 relative to pure X and isolated B atoms in their equilibrium crystal structures [20] and it was evaluated according to (4).

$$\Delta E^{\Theta}(\mathrm{XB_2}) = \frac{1}{3}E^{\Theta}_{\mathrm{XB_2}} - \left[\frac{1}{3}E^{\Phi}_{X} + \frac{2}{3}E^{\psi}_{B}\right], \quad (4)$$

where $\Delta E^{\Theta}_{XB_2}$ is the total energy of XB_2 with Θ structure, E^{Φ}_{X} is the total energy per atom of X with Φ structure and E^{ψ}_{B} is the total energy per atom of B with ψ structure. Negative formation energy indicates a thermodynamically stable material, while a positive one indicates an unstable or metastable material.

3. RESULTS AND DISCUSSION

Calculations were carried out on four different crystal structures – the traditional AlB_2 structure, the monoclinic *C*2/m, the orthorhombic *P*mmn and a cubic structure with the same composition and atomic positions as the AlB_2 structure. Since the cubic structure is hypothetical, three possible atomic position arrangements were investigated. The results are shown in Fig. 2. The celd1 curve is for the arrangement that has X atoms at the (0; 0; 0) positions, celd2 is for the arrangement where X atoms are at $(\frac{1}{3};\frac{1}{6};\frac{1}{2})$ and celd3 is for the arrangement in which X atoms locate at $(\frac{2}{3};\frac{1}{3};\frac{1}{2})$. It is evident from the curves that the most stable arrangement is the ones in which X (metal) atoms locate at the (0; 0; 0) position. Therefore, for both the hexagonal and the cubic noble metal XB_2 (X = Pt, Ir, Rh, Pd) diborides, the X atoms will prefer the (0, 0, 0) position while the two boron atoms will prefer the $(\frac{1}{3};\frac{1}{6};\frac{1}{2})$ and $(\frac{2}{3};\frac{1}{3};\frac{1}{2})$ positions.

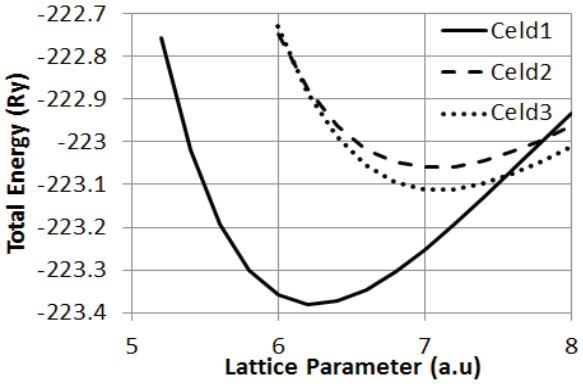

Fig.2. Energy curve for different atomic configuration in the cubic structures of XB_2 (Pt, Ir, Rh, Os, Pd)

The relative energy (E_0) among the phases is given in Table 1. XB_2 (X = Ir, Os, Pt, Rh, Pd) has the lowest energy in the orthorhombic *P*mmn phase. The ground state structure of OsB_2, IrB_2, PtB_2, RhB_2 and PdB_2 is therefore, predicted to be orthorhombic and not cubic, monoclinic or hexagonal. This result agrees with the previous result on OsB_2 [8]. Our result on IrB_2 agrees with the work of Chen et al. [9] but not with that of Binchua et al. [10]. Our result is predicting the orthorhombic *P*mmn structure in PtB_2 and PdB_2 because the E_0 for this phase is much more thermodynamically stable than other phases. Considering the bulk modulus (B_0), it

is important to note the closeness between our calculated results and experimental values for the elemental platinum group metals. The proximity between our calculated values (389.7 GPa) and the experimental values (365--395 GPa) for OsB_2 in the *P*mmn phase gives one the confidence that the bulk moduli are reliable for prediction. Hardness is one of the unique properties of metallic diborides. It is an intrinsic property, difficult to describe with a formal theoretical definition. It can be studied indirectly because it correlates with many physical properties such as ionicity, melting point, elasticity, cohesive energy, etc. The bulk modulus (i. e. material resistance to uniform compression) scales roughly with hardness [20] and it has been used with success to determine hard materials. Based on the bulk modulus results in Table 1, the hardness of the materials are predicted in the order of $RhB_2 > OsB_2 > PdB_2 > IrB_2 > PtB_2$. All values in this range are exceptionally high, exceeding or matching other hard materials, including boron carbide (200 GPa), silicon carbide (248 GPa), sapphire (252 GPa), and c-BN (367 GPa), and almost approaching that of diamond (442 GPa). It is evident from the B_0 results that incompressibility would increase by about 116% when boron (B) is added to Pd, by about 27% when B is added to Pt and about 5.36% when B is added to Rh. Adding boron into Ir and Os would reduce their compressibility by 4.53% and 18.3% respectively.

With regard to the formation energy, ΔE^{Θ}, all the compounds in the *P*mmn structure have negative but lower ΔE^{Θ} compared to the other phases and are predicted to be more thermodynamically stable. Solid solution should be readily formed between boron and Pt, followed by Pd, Ir, Os, and Rh. The electronic density of states (DOS) and the atom resolved partial density of states (PDOS) are crucial to the understanding of physical properties of materials. The DOS and PDOS for the *P*mmn phases of XB_2 (X = Ir, Pt, Os, Rh, Pd) at 0 GPa are shown in Fig. 3. The finite electronic DOS at the Fermi level (zero point on the x-axis) indicates that all the compounds are metallic. The DOS and the atom resolved PDOS for OsB_2, PtB_2 and PdB_2 are similar. Much overlap is seen between the d-electron of Pt, Pd, Os and the p-electron states of boron. Strong covalent bond is predicted in these compounds. No clear overlap is seen between the d- and f-electron states of IrB_2 and RhB_2. For engineering applications, the ability of a material to be machined into sharp edge or complex shapes is important. Borides with low hardness (i.e., hexagonal Boron Nitride and MAX phases) are readily machinable. The machineability of the XB_2 diborides is therefore predicted in the reverse order to their hardness, i.e., IrB_2 and RhB_2 should be more machineable than PtB_2, PdB_2, and OsB_2.

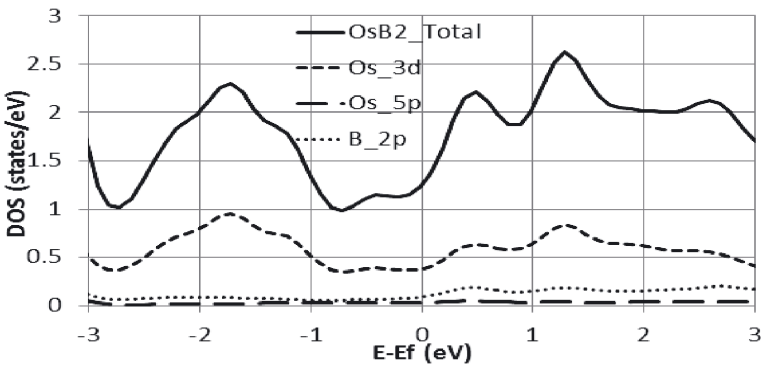

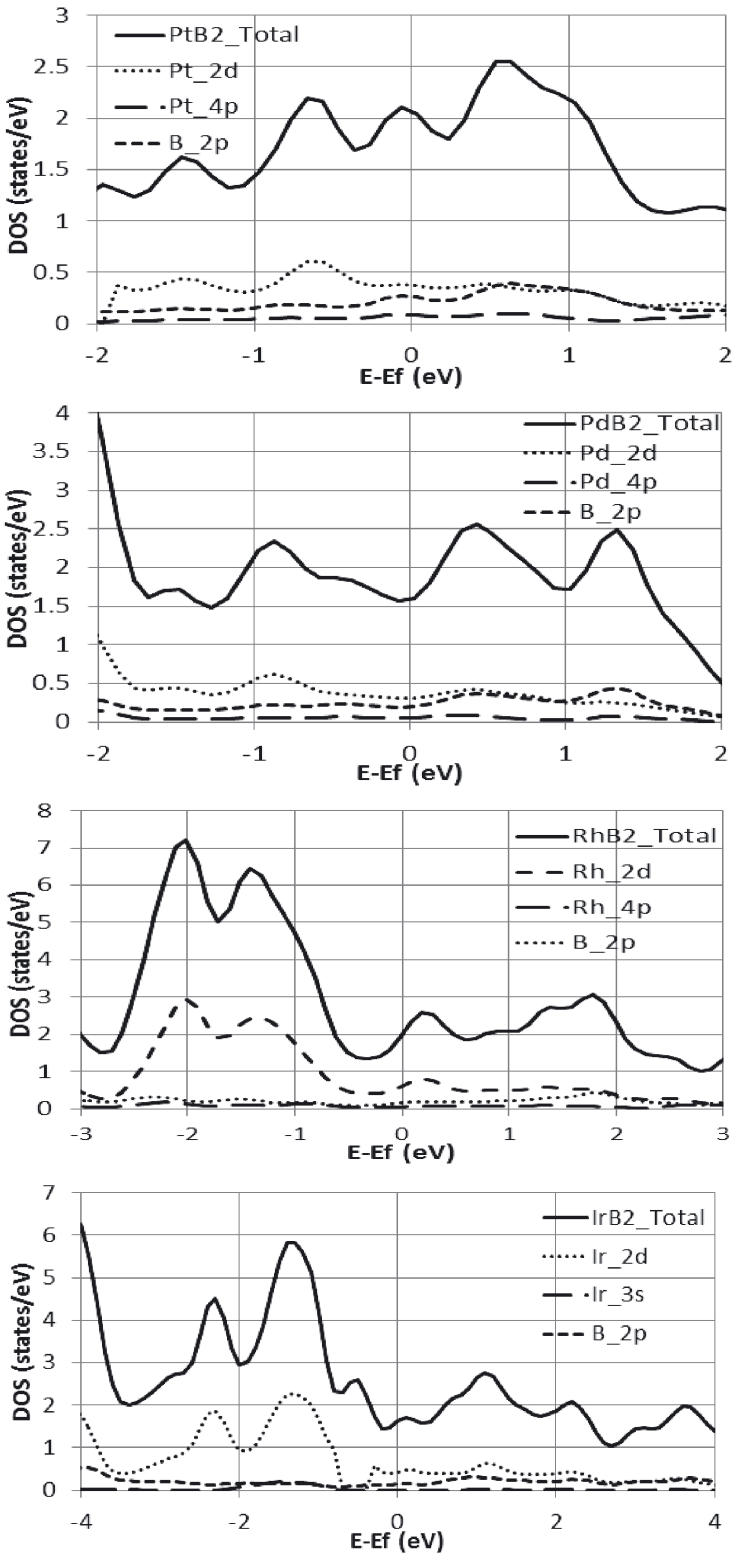

Fig. 3. The total and partial DOS for OsB_2, PtB_2, PdB_2, RhB_2 and IrB_2 in the *P*mmn structure. The Fermi level (on the x-axis) has been shifted to zero point.

Table 1

Calculated Formation Energy (ΔE^{Θ}), Equilibrium Ground State Energy (E_0) and the Bulk Modulus (B_0) for the Elemental Platinum Group Metals, the Cubicγ, Hexagonal‡, Monoclinic^{a} and the Orthorhombic$ Structures of XB_2 (X = Pt, Ir, Os, Pd, Rh)

Mater.	ΔE^{Θ}(Ry)	E_0(Ry)	B (GPa)
Pt	-	-	276.7 [230]
Ir	-	-	379 [320]
Rh	-	-	374 [380]
Pd	-	-	172 [180]
Os	-	-	461 [462]
RhB_2	-129.31γ -133.23‡ -129.15^{a} -313.30$	-183.90γ -187.76‡ -183.68^{a} -367.70$	160.4γ 371.4‡ 341.4^{a} 393.6$
IrB_2	-140.19γ -144.64‡ -140.07^{a} -334.84$	-194.43γ -198.78‡ -194.26^{a} -388.84$	180.4γ 370.2‡ **338.2**^{a} 362.5$
PdB_2	-152.85γ -157.53‡ -152.77^{a} -364.32$	-211.39γ -215.95‡ -211.16^{a} -422.69$	161.1γ 353.7‡ 307.1^{a} 372.1$
PtB_2	-172.45γ -176.43‡ -162.40^{a} -385.10$	-223.38γ -237.22‡ -223.15^{a} -446.72$	183.9γ 374.6‡ 322.8^{a} 352.5$
OsB_2	-103.29γ -107.44‡ -102.99^{a} -314.52$	-211.18γ -215.39‡ -211.02^{a} -422.33$	241.3γ 396.7‡ 347.4^{a} 389.7$ [365-395]

Experimental data in parentheses are from references [8], [21], [22].

4. CONCLUSIONS

Using first-principle calculations based on density functional theory, an orthorhombic *P*mmn structure has been shown to be the ground-state structure for IrB_2, OsB_2, PtB_2, RhB_2, and PdB_2. PtB_2 is the most energetically favoured when compared to the other compounds. It is worth noting that boron will affect the compressibility of Pt, Rh and Pd differently to that of Os and Ir. The compressibility of elemental Os is much higher than for Rh. Surprisingly, boron addition in Rh should lead to much improvement in its compressibility than its addition into Os. According to the

calculated DOS and PDOS, it is concluded that PtB_2, PdB_2, and OsB_2 are potentially incompressible and superhard materials than IrB_2 and RhB_2.

REFERENCES

1. Thornton, A., & Wilks, G. (1978). Clean surface reactions between diamond and steel. *Nature, 274,* 792 – 793.
2. Solozhenko, V. L., Andrault, D., Fiquet, G., Mezouar, M., & Rubie, D. C. (2001). Synthesis of superhard cubic BC_2N. *Appl. Phys. Lett. 78*(10)*,* 1385 - 1387.
3. Haines, J., Léger, J. M., & Bocquillon, G. (2001). Synthesis and Design of Superhard Materials. *Annu. Rev. Mater. Res., 31*(1)*,* 1 - 23.
4. Kaner, R. B., Gilman, J. J., & Tolbert, S. H. (2005). Materials science. Designing superhard materials. *Science, 308,* 1268 - 1269.
5. Hebbache, M., & Zemzemi, M. (2004). Ab initio study of high-pressure behavior of a low compressibility metal and a hard material: Osmium and diamond. *Phys. Rev. B, 70,* 224107.
6. Roof, R. B. Jr., & Kempter, C. P. (1962). New orthorhombic phases in the Ru-B and Os-B. *J. Chem. Phys. 37*(7)*,* 1473 – 1478.
7. Stuparevic, L., & Zivkovic, D. (2004). Phase diagram investigation and thermodynamic study of OsB system. *J. Ther. Anal. Calori., 76*(3)*,* 975 - 983.
8. Cumberland, R. W., Weinberger, M. B., Gilman, J. J., Clark, S. M., Tolbert, S. H., & Kaner, R. B. (2005). Osmium diboride, an ultra-incompressible, hard material. *J. Am. Chem. Soc., 127,* 7264 – 7265.
9. Wang, D. Y., Wang, B., & Wang, Y. X. (2012). New crystal structures of IrB and IrB2: First-principles calculations. *J. Phys. Chem. C, 116,* 21961 – 21966.
10. Chu, B., Li, D., Bao, K., Tian, F., Duan, D., Sha, X., & Cui, T. (2014). The crystal structure of IrB2: A first-principle calculation. *RSC Adv., 4,* 63442 – 63446.
11. Chu, B., Li, D., Bao, K., Tian, F., Duan, D., Sha, X., Liu, Y., & Cui, T. (2015). Structural, mechanical, and electronic properties of Rh_2B and RhB_2: First-principles calculations. *Scientific Reports 5,* doi: 10.1038/srep10500.
12. Wolff, I.M., & Hill, P.J. (2002). Platinum Metals-Based Intermetallics for High-Temperature Service. *Platinum Metals Review, 44*(4)*,* 158 - 166.
13. Haines, J., Léger, J. M., & Atouf, A. (1995). Crystal Structure and Equation of State of Cotunnite-Type Zirconia. *J. Am. Ceram. Soc. 78*(2)*,* 445 - 448.
14. Teter, D.M. (1998). Computational Alchemy: The Search for New Superhard Materials. *Mater. Res. Soc. Bull., 23*(1)*,* 22 - 27.
15. Lundin, U., Fast, L., Nordstrom, L., Johansson, B., Wills, J. M., & Eriksson, O. (1998). Transition-metal dioxides with a bulk modulus comparable to diamond. *Phys. Rev. B, 57,* 4979 - 4982.
16. Giannozzi, P., Baroni, S., Bonini, N., Calandra, M., Car, R., Cavazzoni, C., & Wentzcovitch, R. M. (2009). QUANTUM ESPRESSO: A modular and open-source software project for quantum simulations of materials. *J. Phys: Cond. Matt., 21*(39)*,* 395502.
17. Perdew, J.P., Burke, K., & Ernzerhof, M. (1996). Generalized Gradient Approximation Made Simple. *Physical Review Letters, 77,* 3865.
18. Monkhorst, H.J., & Pack, J.D. (1976). Special points for Brillouin-zone integrations. *Phys. Rev. B, 13,* 5188 – 5192.
19. Birch, F. (1947). Finite Elastic Strain of Cubic Crystal. *Phys. Rev., 71,* 809 - 824.

20. Staple, C., Mannstadt, W., Asahi, R., & Freeman, A.J. (2001). Electronic structure and physical properties of early transition metal mononitrides: Density-functional theory LDA, GGA, and screened-exchange LDA FLAPW calculations. *Phys. Rev. B, 63(15),* 155106(1 - 11).
21. James, A.M. & Lord, M.P. (1992*). Macmillan's Chemical and Physical Data*, London: Macmillan.
22. Kaye, G.W.C. & Laby, T. H. (1993). *Tables of physical and chemical constants* (15th ed.), London: Longman.

XB_2 (X = PT, IR, PD, RH, OS) DIBORĪDU STABILITĀTE UN ELEKTRONISKĀ STRUKTŪRA

A.I. Popoola, A.Y. Odusote, O.E. Ayo-Ojo

Kopsavilkums

Rakstā veikti pirmo principu aprēķini, lai izpētītu platīna grupas metāla diborīdu strukturālās un elektroniskās īpašības stehiometriskā XB_2 (X = Pt, Ir, Pd, Rh, Os). Visi pētītie savienojumi pierādīja, ka tie pieder pie ortorombiskās *P*mmn telpiskās grupas, nevis pie *C2*/m, kas tika iepriekš noteikts dažās kompozīcijās. Saspiežamība samazinās ar bora pievienošanu Pt, Pd un Rh, bet palielinās ar bora pievienošanu Ir un Os. Stāvokļu elektroniskais blīvums parāda, ka visi savienojumi ir metāli, un PtB_2, PdB_2 un OsB_2 ir potenciāli nesaspiežami un supersmagie materiāli.

28.12.2016.